

MATHEMATICAL VISUALIZATION OF THE GENERAL CIRCULATION

Jacques C.J. NIHOUL, S. DJENIDI and E. DELEERSNIJDER
GHER, University of Liège, B-4000 Liège (Belgium)

ABSTRACT

Jacques C.J. Nihoul, S. Djenidi and E. Deleersnijder, 1989
Mathematical visualization of the general circulation

The application of diagnostic-prognostic models to the mathematical visualization of the general circulation and associated (current, buoyancy, nutrient, plankton ...) fields, - primarily apprehended from historical or newly acquired data -, is discussed and illustrated with results of simulation with the GHER model.

INTRODUCTION

Although mesoscale processes - often very intense - like tides and storm surges on the continental shelf, have an obvious effect on the marine system and strongly affect observations, the final interpretation of data and the description of ecological processes require a good understanding of the long term displacement of water masses, the cumulated deposition of sediments, the persistence of upwellings and downwellings and the associated barotropic-baroclinic instabilities. What is needed is a comprehensive synthetic picture of synoptic and macroscale processes which characterize the vertical and horizontal transports and diffusions at, say, monthly or seasonal scales, what one generally refers to as the "general circulation" of the sea.

The determination of macroscale fields of currents, temperature, salinity, nutrients, ... is an experimental puzzle. No matter the scale of the marine system under investigation, ships, buoys and other observation vectors such as remote sensing planes and satellites, can only survey selected tracks during specific periods and for a limited number of state variables.

The result of such a survey, for a particular month or season, will be, in most cases, a fragmentary picture of the system, not really sufficient to form an opinion on its dynamical state and possible vulnerability to pollution.

It is of course possible to compound, for the same month or season, from the recent observations and historical data, - disregarding differences in days (for a given cruise) and in years (for climatic estimates of missing informations) - a more complete image of the system, grossly representing its typical monthly or seasonal features.

Although, for lack of anything better, chemists, biologists, geologists ... have often worked directly from such an image, one must recognize that, even in the best cases, it can be little more than a fuzzy view of the system.

To focus it, one can use a diagnostic-prognostic model.

One must assume that the mean (atmospheric, open-sea boundary ...) forcings are known for the period (a month, a season ...) under consideration. Then, from a given initial state, the model can predict the evolution of the marine system, under these steady forcings, until a "steady" state, - within the precision pertinent to the experimental data and the objectives of the model -, is reached when the system is in equilibrium with its forcings.

Obviously, if one could, from out-of-phase observations during the studied period and historical data for the same period of the year but from different years, guess correctly what the state of the system actually was during that period, one would have the solution of the model's equations which correspond to the associated mean steady forcing.

Because, this is not the case, the model does not accept the constructed initial state as the appropriate permanent solution and forecasts the evolution of the system towards a different, better adapted, configuration. If the initial conditions are not far from reality, the adjustment can be achieved by only a limited number of iterations.

The result of the simulation however is not truly a forecast : scattered results from a given month and climatological data for the same month are used to predict the typical "mean" state of the marine system for that month.

This type of simulation is related to what people call "nowcasting" and also "data assimilation". It will be referred to here as "*mathematical visualization*".

APPLICATION OF $k-\epsilon$ MODELS TO THE DETERMINATION OF THE GENERAL CIRCULATION

To model the general circulation, it is tempting to consider long time averages (several weeks) and, identifying the highlighted macroscale flow with the "mean flow" of $k-\epsilon$ models, treat all smaller scale motions as "fluctuations".

It is doubtful, however, that the parameterization schemes of classical $k-\epsilon$ models can be applied to sub-window scale fluctuations which now include mesoscale processes such as tides and wind-induced currents.

These processes - even if they often appear suitably chaotic thanks to wind variations and long waves' multiple reflections and non-linear interactions - have incommensurable horizontal and vertical characteristics with several orders of magnitude differences in length scales and energy.

The k - ϵ closure is based on arguments inspired by three-dimensional isotropic turbulence and their extension to highly anisotropic mesoscale fluctuations would be foolhardy.

Mesoscale processes are characterized by energetic horizontal motions and large horizontal length scales and, by the continuity equation, weak vertical motions and vertical length scales not exceeding the depth. Small scale turbulence has comparable length scales and velocity scales in the horizontal and in the vertical.

If L_1 and u_1 denote typical horizontal length and velocity scales for mesoscale motions in a shelf sea, the associated vertical velocity scales for mesoscale and turbulent flows are given respectively by (e.g. Nihoul 1975, 1977a,b, 1982 ; Nihoul et al 1989)

$$u_v \sim \frac{u_1 H}{L_1} \quad (\text{mesoscale})$$

(where H is the depth)

$$u_* \sim D^{\frac{1}{2}} u_1 \quad (\text{turbulent})$$

(where D is the drag coefficient). Taking $H \sim 50$ m, $L_1 \sim 10^5$ m, $D \sim 3 \cdot 10^{-3}$, one finds

$$\frac{u_v}{u_*} \sim \frac{H}{L_1 D^{\frac{1}{2}}} \sim 10^{-2}$$

Thus, the vertical mesoscale advection is small and the vertical mixing associated with its variability may be neglected as compared with typical turbulent vertical mixing. The mesoscale fluxes reduce to their horizontal components.

To assess the importance of these fluxes, it is instructing to consider two asymptotic cases :

- (i) a well-mixed shelf sea like the North Sea in the winter where tides are dominant - imposing recurrent structures on the mesoscale flow fields - together with intense storm surges and where mesoscale velocities can be one or two orders of magnitude larger than residual velocities ;
- (ii) a stratified shelf sea like the Northern Bering Sea in the summer where tidal motions are relatively small, wind-induced currents comparatively versatile and where mesoscale velocities are comparable with typical macroscale current speeds.

In the following, the subscript "0" denotes the general circulation while the subscript "1" refers to superimposed mesoscale motions.

In the first case, assuming $u_1 \sim 1 \text{ m s}^{-1}$, $u_0 \sim 10^{-1} \text{ m s}^{-1}$ and taking into account that the relative coherence imposed by the dominant tides maintains the average $(\mathbf{u}_1 \mathbf{u}_1)_0$ a substantial fraction of $\mathbf{u}_1 \mathbf{u}_1$, one can write conservative estimates of $\nabla \cdot (\mathbf{u}_0 \mathbf{u}_0)$, $\nabla \cdot (\mathbf{u}_1 \mathbf{u}_1)_0$, $2\boldsymbol{\Omega} \wedge \mathbf{u}_0$ as

$$\begin{aligned}\nabla \cdot (\mathbf{u}_0 \mathbf{u}_0) &\sim 10^{-7} \\ \nabla \cdot (\mathbf{u}_1 \mathbf{u}_1)_0 &\sim 10^{-5} \\ 2\boldsymbol{\Omega} \wedge \mathbf{u}_0 &\sim 10^{-5}\end{aligned}$$

The mesoscale Reynolds stress is thus an essential forcing of the general circulation (as important as the Coriolis effect) and it must be taken into account as accurately as possible.

In the second case, assuming $u_1 \sim u_0 \sim 3 \cdot 10^{-1} \text{ m s}^{-1}$ and allowing for one order of magnitude difference between $\mathbf{u}_1 \mathbf{u}_1$ and $(\mathbf{u}_1 \mathbf{u}_1)_0$ in the absence of dominant cohesive tidal motions, one finds

$$\begin{aligned}\nabla \cdot (\mathbf{u}_0 \mathbf{u}_0) &\sim 10^{-6} \\ \nabla \cdot (\mathbf{u}_1 \mathbf{u}_1)_0 &\sim 10^{-7} \\ 2\boldsymbol{\Omega} \wedge \mathbf{u}_0 &\sim 3 \cdot 10^{-5}\end{aligned}$$

The mesoscale flux of momentum is thus a relatively small effect and one may argue that it can be parameterized as simple horizontal diffusion. This effect may then be combined with the horizontal sub-grid scale diffusion associated with the horizontal resolution of the numerical grid (Nihoul et al 1989).

A similar approximation may presumably be made for the mesoscale fluxes of buoyancy and turbulent kinetic energy (the comparison is made here between mesoscale diffusion and advection by the general circulation).

To understand the implications of this approximation, it is illuminating to discuss briefly the role of the mesoscale Reynolds stresses in shallow shelf seas satisfying the conditions of case 1. In this case, the mesoscale Reynolds stress tensor is an essential forcing and should be calculated explicitly.

The same would be true, of course, of the corresponding fluxes of buoyancy and turbulent kinetic energy.

Fortunately, the turbulence generated by the intense mesoscale currents destroys the stratification. Then much simpler models (2D, 2D + 1D, ...) may be used, leaving aside completely buoyancy and turbulent kinetic energy (e.g. Nihoul and Djenidi 1987).

On the other hand, the predominance of the energetic mesoscale motions allows their prior determination, independently of the weak residual component. The preliminary forecasts of a few typical mesoscale situations and the collation of the model's results with all available observations provide the necessary data base to compute explicitly, with a sufficient degree of accuracy, the mesoscale Reynolds stress tensor and apply it, as a given forcing, in the equations for the general circulation (Djenidi 1987 ; Nihoul and Djenidi 1987).

In many cases, this additional forcing is found responsible for the appearance, in the general circulation flow pattern, of local secondary flows having the form of gyres, marked by closed stream-lines. These gyres, although disrupted and moved along by tidal currents, contribute nevertheless to increase the residence time of water masses in the area and may significantly affect the transfer of marine contaminants (e.g. Nihoul 1982).

This situation is particularly well illustrated by the results of a simulation of the general circulation and long-term transports of pollutants on the Northwestern European Continental Shelf (Djenidi 1987) (fig. 1).

The boundary conditions impose that, at the air-sea interface, the mean turbulent fluxes of momentum, buoyancy, turbulent energy, ... - allowing for surface sources and sinks - must be continuous.

Because turbulent fluxes are non-linear functions of state variables' differences between air and water (e.g. Nihoul 1975), the mean fluxes cannot be related to mean values of atmospheric and marine quantities. The main contribution is the macroscale average of products of mesoscale fluctuations and this must be evaluated separately from statistics of wind fields, air temperatures and humidities, cloud covers, rainfalls, sea surface temperatures ... over the mesoscale range. The part directly played by macroscale processes is comparatively negligible.

Thus, at the level of the general circulation, air-sea exchanges act as predetermined boundary constraints, independent of the computed macroscale state of the sea.

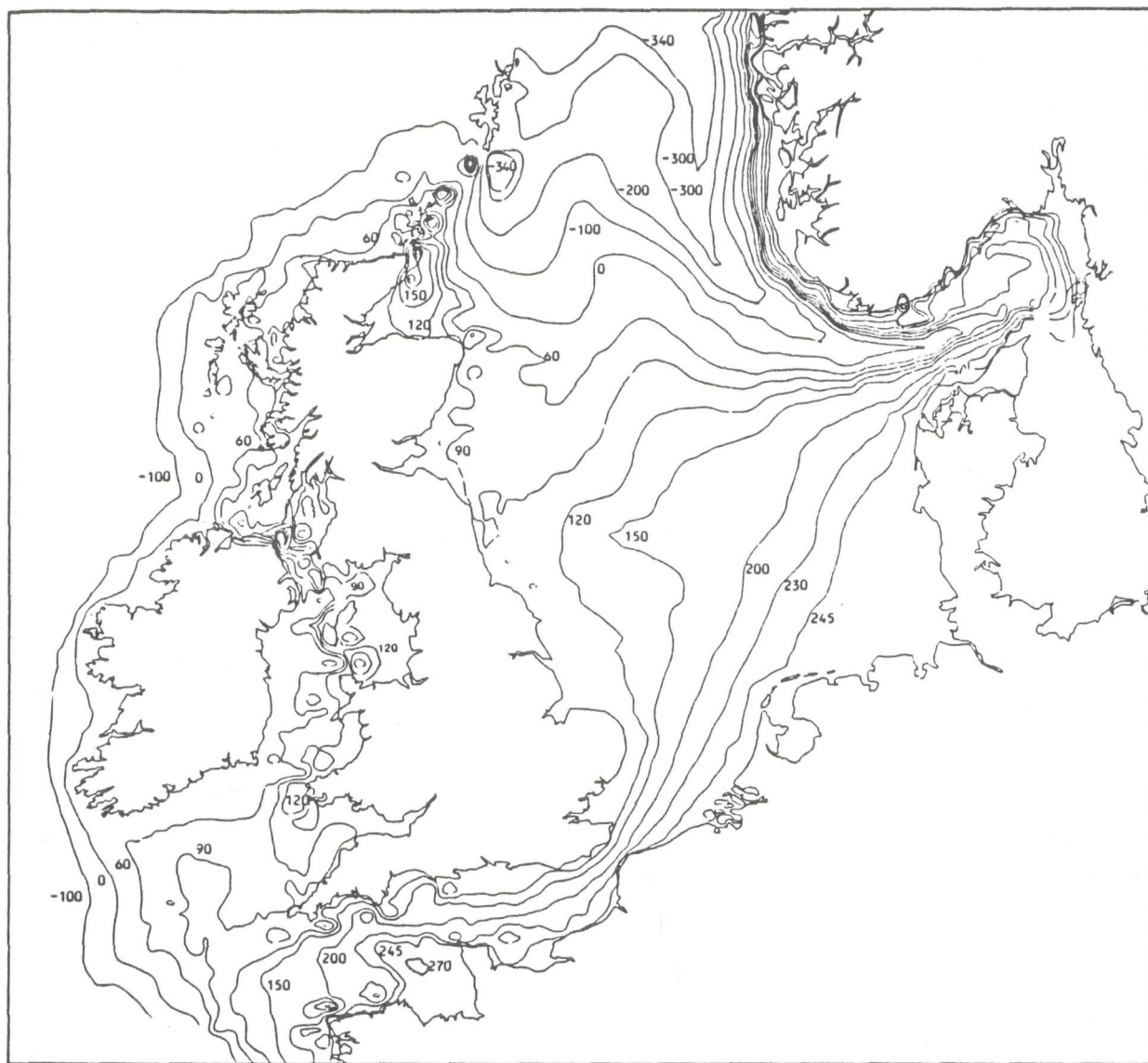


Fig. 1. Streamlines of the depth-integrated circulation (graduated in $10^3 \text{m}^3 \text{s}^{-1}$) on the Northwestern European Continental Shelf with mesoscale Reynolds stress forcing and real wind forcing (typical summer situation).

Another mesoscale effect which is related to air-sea interactions is the contribution of mesoscale transfers of momentum to the production of turbulent kinetic energy in the upper layer of the sea.

In the case of well-mixed shelf seas where simple (depth-integrated) models can be used and the turbulent kinetic energy equation may be dispensed with, the parameterization of the mesoscale energy production rate is not needed but it may play an important role in stratified systems requiring fully three-dimensional models.

An explicit preliminary calculation of this contribution - as for the meso-scale Reynolds stresses in well-mixed tidal seas - does not seem possible in this case but numerous process models of the oceans' mixed layer are available, providing valuable information on the magnitude and depth penetration of transient wind mixing.

As shown by Kitaigorodskii (1979), energy production is maximum in the subsurface layer and decreases rapidly with depth. The total rate of production (integrated over depth) is of the order of $\beta \tau_w^{3/2}$ where τ_w is the wind stress (per unit mass of sea water) and $\beta \sim 10$.

THE GHER 3D GENERAL CIRCULATION MODEL

The three-dimensional model developed at the GeoHydrodynamics and Environment Research Laboratory (GHER) of the University of Liège has been described in various earlier publications (e.g. Nihoul et al 1989).

In the version of the model appropriate to the study of the general circulation in shelf seas, the state variables are the three components of the velocity vector \mathbf{u} , the pressure (or $q = p/\rho + gx_3$), the buoyancy a and the turbulent kinetic energy k .

The mesoscale horizontal Reynolds stresses and fluxes of buoyancy and energy are taken into account in global horizontal diffusion terms which also include sub-grid scale diffusion and the small contribution of small scale turbulence. The horizontal diffusivities are assumed constant (but their values may be functions of the size of the mesh).

Vertical turbulent fluxes are assumed proportional to the vertical gradients of the mean fields' characteristics and the diffusivity coefficients are related to the mixing length ℓ_m and the turbulent kinetic energy. The mixing length is a function of depth and of the flux Richardson number.

The mesoscale energy production rate is written

$$\pi = \langle \{-\mathbf{w} \mathbf{w}\} : \nabla \mathbf{u}_1 \rangle_0 \sim \tilde{\beta} [\tau_w^{3/2}]_0 \quad (1)$$

where $\tilde{\beta}$ is also a function of the depth and the flux Richardson number.

The boundary conditions are calculated from statistics of wind fields, air temperatures and humidities, cloud covers, rainfalls, sea surface temperatures ... over the mesoscale range (The part directly played by macroscale processes is comparatively negligible). The basic equations may be written as follows

$$\frac{\partial u_1}{\partial x_1} + \frac{\partial u_2}{\partial x_2} + \frac{\partial u_3}{\partial x_3} = 0 \quad (2)$$

$$\frac{\partial u_1}{\partial t} + \nabla \cdot (\mathbf{u} u_1) - f u_2 = -\frac{\partial q}{\partial x_1} + \tilde{\mu} \Delta u_1 + \frac{\partial}{\partial x_3} \left(\tilde{\nu} \frac{\partial u_1}{\partial x_3} \right) \quad (3)$$

$$\frac{\partial u_2}{\partial t} + \nabla \cdot (\mathbf{u} u_2) - f u_1 = -\frac{\partial q}{\partial x_2} + \tilde{\mu} \Delta u_2 + \frac{\partial}{\partial x_3} \left(\tilde{\nu} \frac{\partial u_2}{\partial x_3} \right) \quad (4)$$

$$\frac{\partial q}{\partial x_3} = a \quad (5)$$

$$\frac{\partial a}{\partial t} + \nabla \cdot (\mathbf{u} a) = \tilde{\mu}^a \Delta a + \frac{\partial}{\partial x_3} \left(\tilde{\nu}^a \frac{\partial a}{\partial x_3} \right) \quad (6)$$

$$\frac{\partial k}{\partial t} + \nabla \cdot (\mathbf{u} k) = Q^k + \tilde{\mu}^k \Delta k + \frac{\partial}{\partial x_3} \left(\tilde{\nu}^k \frac{\partial k}{\partial x_3} \right) \quad (7)$$

where f is twice the vertical component of the Earth's rotation vector, $\tilde{\mu}$ is the horizontal (mesoscale + turbulent) viscosity, $\tilde{\nu}$ the vertical turbulent viscosity, $\tilde{\mu}^a$ and $\tilde{\mu}^k$ respectively the horizontal (mesoscale + turbulent) diffusivities of buoyancy and turbulent kinetic energy, $\tilde{\nu}^a$ and $\tilde{\nu}^k$, respectively the vertical turbulent diffusivities of buoyancy and energy and where

$$Q^k = \tilde{\nu} \frac{\partial \mathbf{u}}{\partial x_3} \cdot \frac{\partial \mathbf{u}}{\partial x_3} + \pi - \tilde{\nu}^a \frac{\partial a}{\partial x_3} - \varepsilon \quad (8)$$

(with π given by Equation 1).
 ε is the turbulent dissipation rate.

$$\Delta = \frac{\partial^2}{\partial x_1^2} + \frac{\partial^2}{\partial x_2^2} \quad (9)$$

It is assumed that

$$\tilde{\mu}^a = \alpha^a \tilde{\mu} \quad , \quad \tilde{\mu}^k = \alpha^k \tilde{\mu} \quad (10) \quad (11)$$

$$\tilde{\nu}^a = \psi^a \tilde{\nu} \quad , \quad \tilde{\nu}^k = \psi^k \tilde{\nu} \quad (12) \quad (13)$$

$$\tilde{\nu} = 0.5 \alpha^{1/4} \ell_m k^{1/2} \quad (14)$$

$$\varepsilon = \alpha k^2 (16 \tilde{\nu})^{-1} \quad (15)$$

where α , α^a , α^k and ψ^k are taken as constants of order 1 and ψ^a is a function of the flux Richardson number.

$$R_f = \frac{\tilde{\nu}^a \left| \frac{\partial a}{\partial x_3} \right|}{\tilde{\nu} \left\| \frac{\partial \mathbf{u}}{\partial x_2} \right\|^2 + \pi} \quad (16)$$

The model is closed by providing suitable empirical expressions for $\ell_m(x_3, R_f)$, $\beta(x_3, R_f)$ and $\psi^a(x_3, R_f)$, using (historical or specific) data and theoretical results and taking into account the requirements of the numerical scheme (e.g. Nihoul 1977b, Nihoul and Djenidi 1987, Deleersnijder and Nihoul 1988, Nihoul et al 1989).

MATHEMATICAL VISUALIZATION OF THE NORTHERN BERING SEA'S GENERAL CIRCULATION

The Northern Bering Sea is a relatively shallow basin limited by the Bering Strait to the north and St Lawrence Island to the south. The flow passing through the Bering Strait, from the Pacific Ocean to the Arctic Ocean, penetrates the Northern Bering Sea through the Strait of Anadyr, to the west of St Lawrence Island, and by the Strait of Shpanberg, to the east. More than 60% of the mean northward transport of water through the Bering Strait is derived from the "Anadyr Stream", a subsidiary of the Bering Slope Current which flows around the coasts of the Gulf of Anadyr, following the 60-70 isobaths, to the Anadyr Strait.

An extensive survey of the Northern Bering Sea was carried on for five years in the scope of the NSF ISHTAR Program. The observations were concentrated in the summer months with the objective of determining the main physical, chemical and biological characteristics of the system in typical summer situations.

The data were exploited, - together with historical and climatic data (e.g. Coachman et al 1975) -, in simulation exercises, using the GHER 3D Model, aimed at the mathematical visualization of the general circulation in the Northern Bering Sea in the summer.

Figure 2 shows the total transport. One can see the essential contribution of the "Anadyr Stream" flowing in through the Anadyr Strait and deploying in the Northern Bering Sea in agreement with the observations.

Another, extremely interesting, product of the model is the determination of vertical velocities. Horizontal fields of the vertical velocity at different depths show marked upwellings and downwellings reflected in the horizontal and vertical buoyancy distributions.

Figure 3 represents, above, the buoyancy field at 5 m depth. Regions of upwelling (along the Siberian coast and the east coast of St Lawrence Island) are indicated by large negative values at the surface. Vertical advection and mixing in the Anadyr Strait are illustrated by the cross section distributions of buoyancy, below.

Horizontal distributions of buoyancy display non-negligible horizontal gradients and suggest the co-existence of different water masses. Schematically, one can discern three regions : the Anadyr stream drawing along the nutrient-rich upwelled water of the Anadyr Strait into the Northern Bering and Chukchi seas, the Alaskan coastal waters filling the shallow eastern part and presumably overflowing the Anadyr Stream in the central region, an analogous riverine-influenced water mass off the Soviet coast denoted Siberian coastal water.

The separations between water masses have more or less pronounced frontal characteristics. The eastern front is the seat of occasional baroclinic instabilities giving rise to strong secondary flows in the form of eastwards propagating interleaving layers (Nihoul 1986). These layers which have typically a width of 10 km, in the early stages of development, widen progressively as they flow eastwards, spreading the nutrient rich water over the Northern Bering Sea.

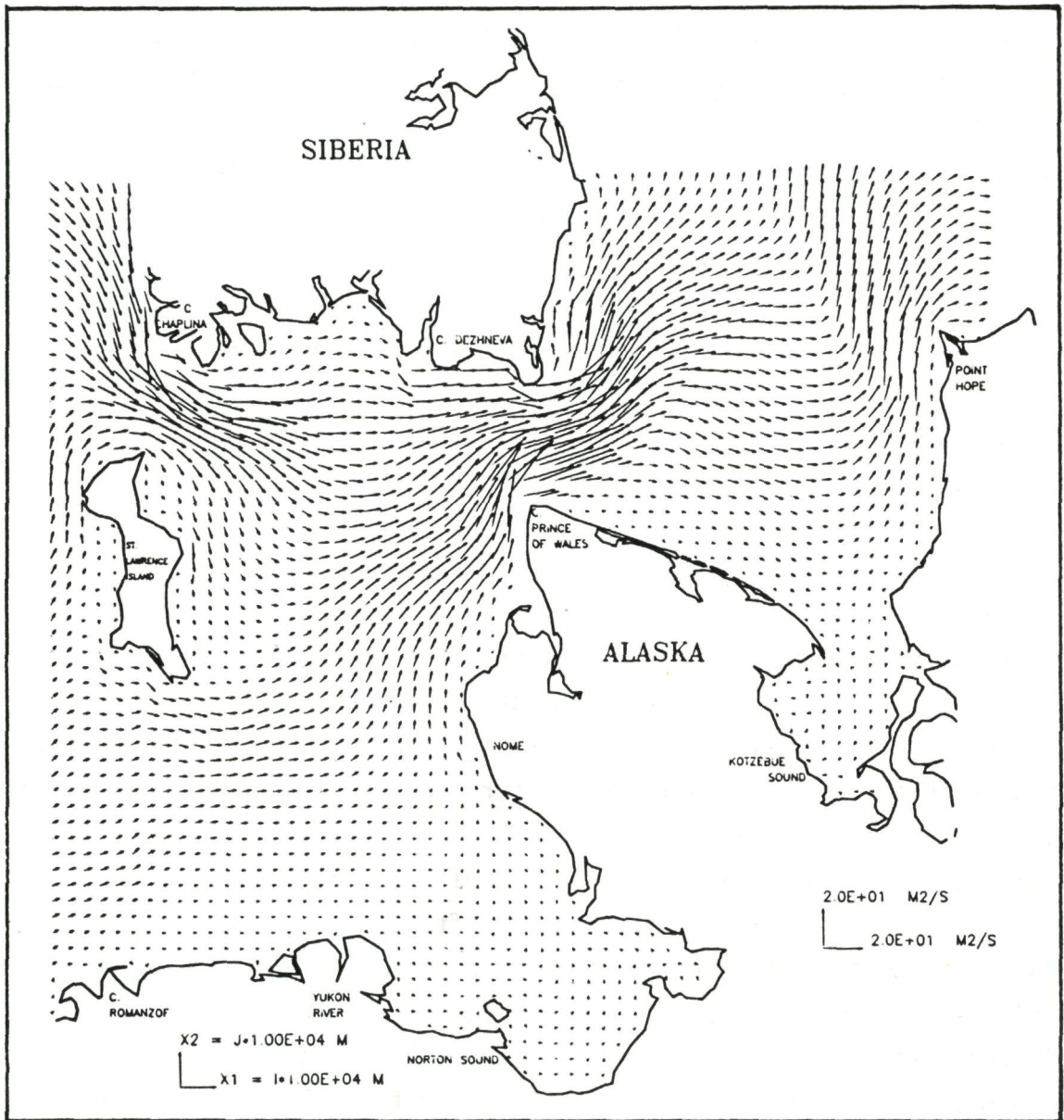


Fig. 2. General summer circulation in the Northern Bering Sea (1.8 Sv through Bering Strait). Total transport calculated by the 3D model (m^2/s). One can see the essential contribution of the "Anadyr Stream" flowing in through the Anadyr Strait (West of St Lawrence Island) and deploying in the Northern Bering Sea.

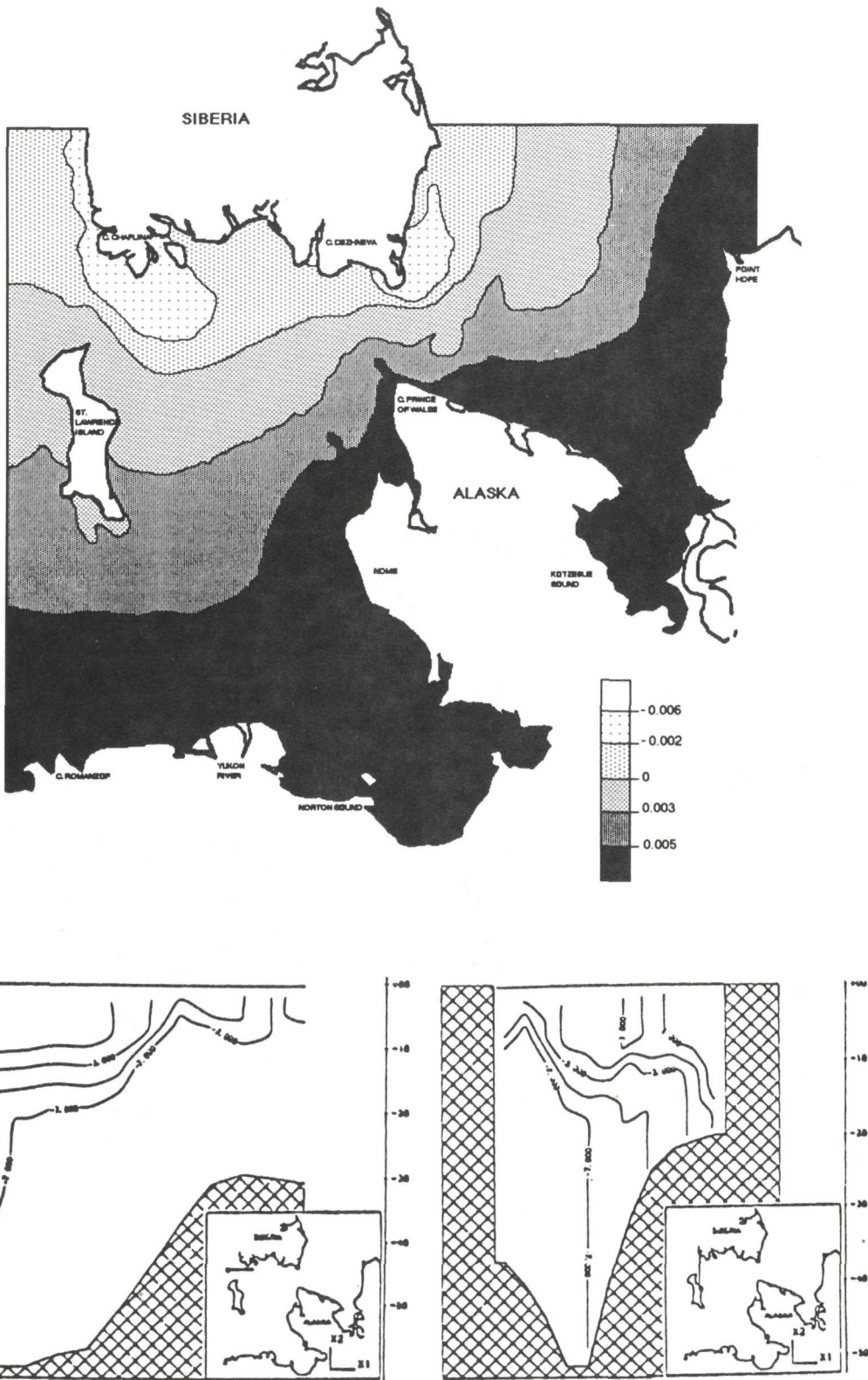


Fig. 3. Buoyancy field at 5 m depth in the Northern Bering Sea (above). Distribution of buoyancy in two sections across the Anadyr Strait.

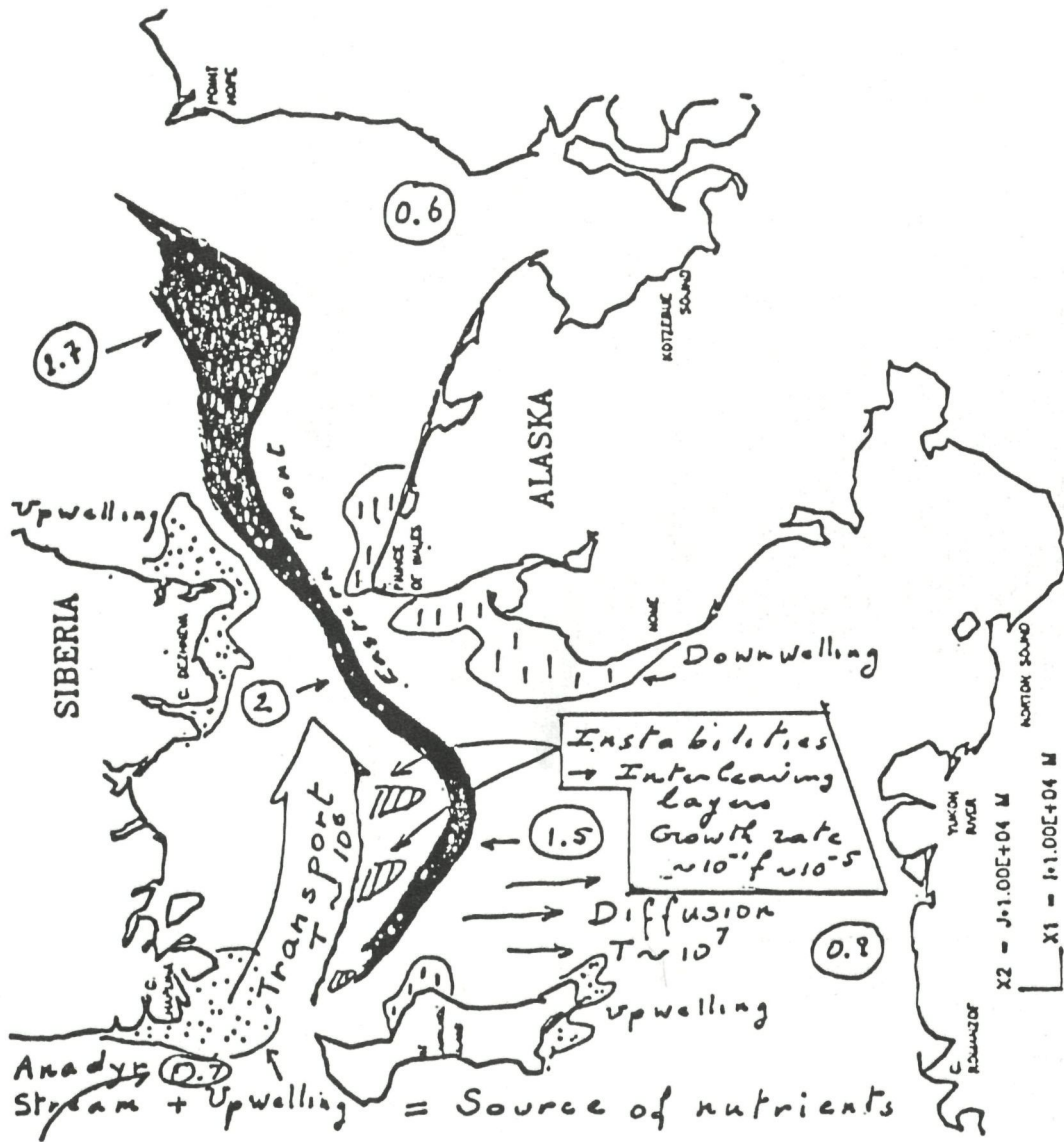


Fig. 4. Cartoon of the ecohydrodynamics of the Bering Sea. [The figures in the circles are the total (ammonium, urea and nitrate) integrated nitrogen uptake rates ($\text{mg-at N m}^{-2} \text{hr}^{-1}$) during the summer 1987].

The formation of such layers can be explained by a baroclinic instability of the cold plume's frontal edge. Using the numerical results of the 3D Model, the stability analysis give the characteristics of the incipient layers in good agreement with the observations (Nihoul 1986).

It is illuminating to interpret the frontal system of the Northern Bering Sea in terms of ergocline ecohydrodynamics. The growth rate of the frontal instabilities may be estimated by the model as being of the order of $10^{-1}f$ i.e. $10^{-5} s^{-1}$. The characteristic time one may thus associate with the development of the extruding layers is of the order of 10^5s and comparable with typical time scales of phytoplankton growth, while horizontal transport and diffusion have much larger time scales. The tuning between the plankton dynamics and the secondary flow constituted by the nutrient rich extruding layers may explain the high productivity associated with the eastern front (Walsh et al 1989) as shown in the cartoon presented in figure 4.

The few examples presented in this paper show how mathematical visualization may help to organize incomplete data to provide a focused view of the general circulation and the associated ecohydrodynamics of shelf seas.

ACKNOWLEDGMENTS

The author acknowledges with gratitude the supports of the National Science Foundation (USA) and of the Ministry for Science Policy (Belgium). He is indebted to the National Fund for Scientific Research (Belgium) for providing supercomputer facilities.

REFERENCES

- Coachman, L.K., Aagaard, K. and Tripp, R.B., 1975. Bering Strait. The Regional and Physical Oceanography. Univ. of Washington Press, 172 pp.
- Deleersnijder, E. and Nihoul, J.C.J., 1988. General circulation in the Northern Bering Sea. ISHTAR Annual Progress Report, 392 pp.
- Djenidi, S., 1987. Modèles mathématiques et dynamique des mers continentales d'Europe Septentrionale. Ph. Dissertation, Liège University, 218 pp.
- Kitaigorodskii, S.A., 1979. Review of the theories of wind-mixed layer deepening. In : J.C.J. Nihoul (ed.), Marine Forecasting, Elsevier Publ. Co., Amsterdam, 1-33.
- Nihoul, J.C.J., 1975. Modelling of Marine Systems. Elsevier Publ. Co., Amsterdam, 272 pp.
- Nihoul, J.C.J., 1977a. Modèles mathématiques et dynamique de l'environnement. ELE, Liège, 198 pp.
- Nihoul, J.C.J., 1977b. Three-dimensional model of tides and storm surges in shallow well-mixed continental seas. Dyn. Atmos. Ocean., 2: 29-47
- Nihoul, J.C.J., 1982. Hydrodynamic models of shallow continental seas. E. Riga Publ., Liège, 198 pp.

- Nihoul, J.C.J., 1986. Aspects of the Northern Bering Sea Ecohydrodynamics. In : J.C.J. Nihoul (ed.), Marine Interfaces Ecohydrodynamics, Elsevier Publ. Co., Amsterdam, 385-399.
- Nihoul, J.C.J., Deleersnijder, E. and Djenidi, S., 1989. Modelling the general circulation of shelf seas by 3D k- ϵ models. Earth Science Reviews, to be published.
- Nihoul, J.C.J. and Djenidi, S., 1987. Perspective in three-dimensional modeling of the marine system. In : J.C.J. Nihoul and B.M. Jamart (eds), Three-dimensional Models of Marine and Estuarine Dynamics, Elsevier Science Publ. Co., Amsterdam, 1-34.
- Walsh, J.J., McRoy, C.P., Coachman, L.K., Goering, J.J., Nihoul, J.C.J., Whitledge, T.E., Blackburn, T.H., Parker, P.L., Wirick, C.D., Shuert, P.G., Grebmeier, J.M., Springer, A.M., Tripp, R.D., Hensell, D., Djenidi, S., Deleersnijder, E., Henriksen, K., Lund, B.A., Andersen, P., Muller-Karger, F.E. and Dean, K., 1989. Carbon and nitrogen cycling within the Bering/Chukchi Seas : source regions for organic matter effecting AOU demands of the Arctic Ocean. Progress in Oceanography, to be published.